

# Alkali production from bipolar membrane electro dialysis powered by microbial fuel cell and application for biogas upgrading

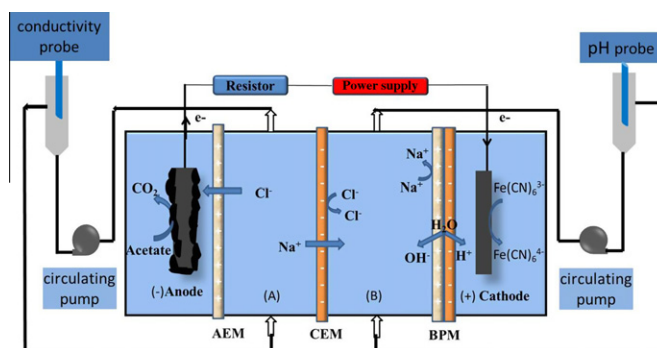
Man Chen<sup>1</sup>, Fang Zhang<sup>1</sup>, Yan Zhang, Raymond J. Zeng<sup>\*</sup>

Department of Chemistry, University of Science and Technology of China, Hefei, Anhui 230026, People's Republic of China

## HIGHLIGHTS

- ▶ BP MED powered by MFC was proposed to utilize electricity *in situ* and produce NaOH.
- ▶ The maximum pH was about 11.6 with 0.5 V applied voltage.
- ▶ The produced NaOH was suitable for biogas upgrading and the final CH<sub>4</sub> reached 100%.
- ▶ The study provides an elegant and sustainable way to extend BP MED & MFC application.

## GRAPHICAL ABSTRACT



## ARTICLE INFO

### Article history:

Received 4 June 2012

Received in revised form 4 September 2012

Accepted 1 October 2012

Available online 9 November 2012

### Keywords:

Microbial fuel cell  
Bipolar membrane electro dialysis  
Electricity *in situ* utilization  
Alkali production  
Biogas upgrading

## ABSTRACT

The biogas upgrading is necessary for its application, and alkali CO<sub>2</sub> adsorption is one efficient method. In this study, a coupled system, bipolar membrane electro dialysis (BP MED)–microbial fuel cell (MFC), was proposed for alkali production, which could also realize electricity *in situ* utilization. It was found that the pH in the alkali production chamber was 9.8. With higher NaCl concentration, bigger applied voltage and lower external resistance, the pH of the produced alkali solution also increased and the maximum value of which was 11.6. Meanwhile, our system also performed desalination. Furthermore, the produced alkali solution was utilized for biogas upgrading. The CO<sub>2</sub> content decreased notably in headspace, which even reached 0% at pH 11.6 of alkali solution. This study provides an elegant and sustainable way to extend BP MED and MFC application.

© 2012 Elsevier Ltd. All rights reserved.

## 1. Introduction

The biogas, which could be maturely produced from renewable biomass and organic wastes in anaerobic digestion, is an alternative energy source for humans [1–3]. It normally consists of 40–75% methane, 25–60% carbon dioxide and other trace gases (for example, H<sub>2</sub>S) [1,3]. The produced biogas should be upgraded for its utilization [4]. For example, as demonstrated by Deng and

Hägg, upgrading methane concentration to 90% could not only efficiently increase its heating value but also notably reduce the acid gas corrosion [5]. The upgraded biogas (>98%) could be compressed and liquefied as vehicle fuel and produce heat and electricity [5]. Meanwhile, the existing natural gas grid could also be utilized for the upgraded biogas transportation. Thereby, the removal of CO<sub>2</sub> is a critical step to utilize biogas.

The common and commercialized methods for CO<sub>2</sub> removal include pressure swing adsorption (PSA), water scrubbing, chemical adsorption, membrane based gas separation, etc. [4,6,7]. Since the additional upgrading operation increases to the costs of biogas utilization, it is important to have an optimized process with low

<sup>\*</sup> Corresponding author. Tel./fax: +86 551 3600203.

E-mail address: [rzeng@ustc.edu.cn](mailto:rzeng@ustc.edu.cn) (R.J. Zeng).

<sup>1</sup> These authors contributed equally to this work.

energy consumption and high efficiency. The chemical adsorption is one efficient way that is characterized of lower working pressure, smaller electricity consumption and higher operating capacity [4,8]. Moreover, the alkali adsorption (such as NaOH) could simultaneously reduce  $\text{CO}_2$  and  $\text{H}_2\text{S}$  and avoid the pre-cleaning of  $\text{H}_2\text{S}$  in PSA and amine scrubber. However, the transporting cost of alkali is one of the issues for its utilization [8]. Therefore, it shall be much better if alkali can be produced on site. Bipolar membrane electrodialysis (BPMED) is an integrated technique of bipolar membrane (BPM) and traditional electrodialysis (ED), which has gained more attentions in the last two decades [9]. Bipolar membrane is a functional composite membrane comprising a cation exchange layer and an anion exchange layer, and can dissociate water into  $\text{H}^+$  and  $\text{OH}^-$  simultaneously between the two layers under reverse bias direct current field [10,11]. Thus, BPMED can produce acid and alkali *in situ* (such as  $\text{H}_2\text{SO}_4$  and NaOH production from  $\text{Na}_2\text{SO}_4$ ), and significantly reduce the cost of acid and alkali [9,12]. Recently, BPMED was also reported to separate and enrich  $\text{CO}_2$  by the *in situ* NaOH production [13]. However, similar to traditional electrodialysis, the investment cost of BPMED is also high [9,14]. Therefore, alkali production from BPMED would be an attractive technology for biogas upgrading if the energy cost could be reduced.

Microbial fuel cell (MFC) has been demonstrated as the novel biotechnology for energy recovery, wastewater treatment, bioremediation and valuable chemicals production [15,16]. In MFC, the bio-convertible substrates are consumed by exoelectrogenic bacteria in anodic chamber to generate proton and electron simultaneously. The proton migrates through proton/cation exchange membrane to the cathodic chamber. And the generated electron transfers through the external resistance to cathode and is consumed by electron acceptors in cathodic chamber [16]. Moreover, some new concepts are proposed to realize the *in situ* utilization of the generated electricity from MFC, such as microbial electrolysis cell, microbial desalination cell, and microbial electrosynthesis [15,17]. Hereby, why not power BPMED by MFC?

It was reported that, acidification (pH decreased from 7.0 to 5.4) in anodic solution and alkalization (pH increased from 7.0 to 9.5) in cathodic solution occur in MFC [18]. The pH changing significantly affected the electrode potential and decreases the voltage and power density of MFC [19]. Consequently, BPM was proposed as the separator in MFC to maintain neutral pH in anodic and cathodic

chambers [20,21]. However, neutral pH was not maintained well because of low water dissociation efficiency of BPM (about 70%) [21,22]. Meanwhile, the high polarization resistance of BPM also led to lower voltage and power density of MFC, which was another drawback for BPM application [23].

Though BPM was not an ideal separator to maintain neutral pH, it can be a functional membrane to produce acid and alkali in MFC. Recently, as proposed by Chen et al. [24], BPM integrated with MFC was successfully used to produce acid and desalt. Therefore, in this study, BPMED was proposed to integrate with MFC to realize alkali production, and then the produced alkali was utilized for biogas upgrading. The parameters, including electrolyte concentration, external resistance, applied voltage and the system configuration, were investigated for alkali production. Then the produced alkali was applied to reduce  $\text{CO}_2$  content in biogas.

## 2. Materials and methods

### 2.1. The setup of BPMED–MFC

As shown in Fig. 1, the whole reactor (AEM–CEM–BPM configuration; AEM, anion exchange membrane; CEM, cation exchange membrane) was separated to four chambers, including anodic chamber, desalination chamber, alkali production chamber and cathodic chamber. Three separators were arranged from left to right in MFC as follows, AEM (AMI-7001, Membranes International Inc., New Jersey), CEM (CMI-7000, Membranes International Inc., New Jersey) and BPM (BPM-1, Tingrun membrane technology development Co. Ltd., Beijing). For AEM–BPM configuration, as the CEM was not used between AEM and BPM, desalination and alkali production were in the same chamber. Hereinafter, the AEM–CEM–BPM configuration would be utilized throughout our study except the case of AEM–BPM configuration. The working area of three kinds of membrane were about  $7\text{ cm}^2$ . The working volume of anodic, cathodic, alkali production and desalination chambers was 40, 40, 60 and 60 mL, respectively. The negative lead of the power supply (DF1731SD2A, Zhongce Electronics Co. Ltd., Ningbo) was connected to the cathode, and an external resistance ( $10\ \Omega$ ) was connected between the positive lead of the power supply and the anode (Fig. 1). Liquid circulation was applied in desalination and alkali production chambers.

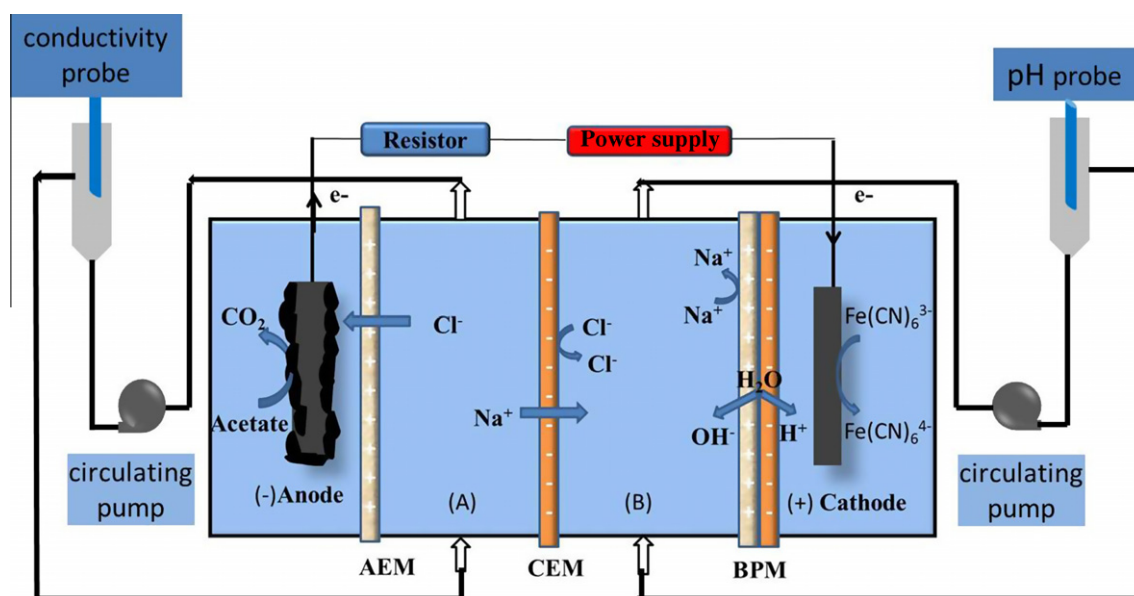


Fig. 1. The AEM–CEM–BPM setup of BPMED–MFC Notes: (A), desalination chamber and (B), alkali production chamber.

## 2.2. The operation of BPMED–MFC

The MFC was inoculated with 10 mL anaerobic sludge collected from the local wastewater treatment plant. The anodic chamber was filled with medium (in 1 L of 50 mM phosphate buffer solution, pH 7.0), which contained acetate sodium, 1200 mg;  $\text{NH}_4\text{Cl}$ , 310 mg; KCl, 130 mg;  $\text{CaCl}_2$ , 10 mg;  $\text{MgCl}_2 \cdot 6\text{H}_2\text{O}$ , 20 mg; NaCl, 2 mg;  $\text{FeCl}_2$ , 5 mg;  $\text{CoCl}_2 \cdot 2\text{H}_2\text{O}$ , 1 mg;  $\text{MnCl}_2 \cdot 4\text{H}_2\text{O}$ , 1 mg;  $\text{AlCl}_3$ , 0.5 mg;  $(\text{NH}_4)_6\text{Mo}_7\text{O}_{24}$ , 3 mg;  $\text{H}_3\text{BO}_3$ , 1 mg;  $\text{NiCl}_2 \cdot 6\text{H}_2\text{O}$ , 0.1 mg;  $\text{CuSO}_4 \cdot 5\text{H}_2\text{O}$ , 1 mg;  $\text{ZnCl}_2$ , 1 mg. The cathodic chamber was filled with 50 mmol/L potassium ferricyanide (in 50 mmol/L phosphate buffer solution, pH 7.0). The initial NaCl concentration was 2 g/L in desalination and alkali production chambers, and the pH was 7.0. The carbon fiber felt (2 cm × 2 cm × 0.2 cm, Sanye Carbon Co. Ltd, Beijing) was used as anodic and cathodic electrodes. The MFC was operated in batch mode at 30 °C, and each experiment was repeated at least twice. The medium in four chambers was replaced with fresh one at the end of each experiment. In control experiments, the only difference was no acetate addition.

## 2.3. Analysis for BPMED–MFC

The concentration of NaCl in desalination chamber was calculated from the conductivity which was measured by conductivity meter (Bante instrument Co., China). The concentration of  $\text{Na}^+$  and  $\text{K}^+$  in alkali production chamber were measured by inductively coupled plasma-optical emission spectrometry (ICP-OES, Thermo Jarrell Ash Co., USA). The concentration of  $\text{Cl}^-$  in alkali production chamber was determined by ion Chromatography (ICS-1000, Dionex, USA). Phosphate ( $\text{HPO}_4^{2-} - \text{P}$ ) in alkali production chamber was determined by Aquakem 200 analyzer (ThermoFisher, Finland). The pH was determined by pH meter. The voltage of the resistor was determined with multimeter and recorded manually.

The concentration of acetate was determined by Agilent 7890 N with a flame ionization detector and a 10 m × 0.53 mm HP-FFAP fused-silica capillary column. The temperature profile of the column was: 70 °C for 3 min, 10 °C/min to 180 °C, hold for 4.5 min. The injector and detector temperature were 250 °C and 300 °C, respectively. The samples were filtered with 0.45  $\mu\text{m}$  microfilter membrane and acidified by 3% (v/v) formic acid before analysis.

The resistance of AEM–CEM–BPM configuration of BPMED–MFC was determined using an electrochemical impedance spectroscopy (EIS) with CHI660C electrochemical workstation (Chenhua Instrument Co., China) at a frequency range from  $10^5$  to 0.01 Hz (two-electrode-setup system), and the amplitude was 0.005 V. Power density and polarization curves were generated via changing the external resistance of AEM–CEM–BPM configuration of BPMED–MFC from 10000  $\Omega$  to 10  $\Omega$  [16], and the system was stabilized at least 0.5 h for each external resistance. The calculation of coulombic efficiency was according to the method of Logan et al. that was based on the acetate changed in the anodic chamber and the current production during the experiment [16]. As shown in Eq. (1),  $I$  is the current of MFC, A;  $F$  is Faraday constant (96,485 C/electron equivalent);  $M$  is the molecular weight of acetate;  $V$  is the volume of liquid in the anode chamber, 0.04 L; and the  $\Delta C$  is the changes in acetate concentration in anodic chamber.

$$\text{CE} = \frac{\int I dt}{8 \times F \times V \times \Delta C / M} \quad (1)$$

## 2.4. Biogas upgrading by alkali solution

The biogas upgrading experiments were performed at five serum bottles (B0, B1, B2, B3 and B4) with the produced alkali

solution under different initial pH (7.0, 9.6, 10.4, 11.2 and 11.6). The working volume was 100 mL and the headspace was 20 mL. After addition of 100 mL above alkali solution, the bottles were sealed with butyl-rubber stopper and aluminum cap, and then the vacuum air pump was used to decrease the headspace pressure below 0.01 atm. 20 mL biogas (60% methane and 40% carbon dioxide) was injected into the above serum bottles. After that, the serum bottles were shaken at 300 rpm at 30 °C. After 20 min, the  $\text{CO}_2$  and  $\text{CH}_4$  were determined by Gas Chromatograph (Lunan model SP7890, China) equipped with a thermal conductivity detector and a 1.5 m stainless steel column packed with 5 Å molecular sieve. The temperature of the injector, detector, and column was kept at 170 °C, 170 °C, and 150 °C, respectively.  $\text{H}_2$  was used as the carrier gas. Each experiment was carried out twice.

## 3. Results

### 3.1. The alkali production and desalination performance in BPMED–MFC

The microbial community in anodic chamber was acclimatized about three weeks before the experiments. The open-circuit potential of AEM–CEM–BPM configuration reactor was about 0.7 V, which was close to the normal MFC [17]. As shown in Fig. 2A, the pH in alkali production chamber increased from 7.2 to 9.8 in the first run as time elapsing. In the second run, the maximum pH was 9.5. Therefore, water dissociation occurred in the BPMED powered by MFC. After reaching the maximum value, pH value decreased gradually to 8.1 in the first run and 7.9 in the second run. Meanwhile, as no substrate was added, the pH in the alkali production chamber of control experiment did not change notably. During the experimental period, the pH in anodic chamber decreased slightly from  $7.0 \pm 0.1$  to  $6.4 \pm 0.2$ .

As shown in Fig. 2B, the current density of MFC decreased from 0.30 to 0.13  $\text{mA}/\text{cm}^2$  in the first, and from 0.34 to 0.17  $\text{mA}/\text{cm}^2$  in the second run. The initial internal resistance of AEM–CEM–BPM configuration was 86  $\Omega$ . However, when water dissociation occurred in BPM, the polarization resistance should significantly increase [25]. Therefore, the current density of BPMED–MFC was lower than that of normal MFC. Meanwhile, the substrate consumption (acetate concentration decreased from 1.1 to 0.4 g/L in the first run), pH decreasing (from  $7.0 \pm 0.1$  to  $6.4 \pm 0.2$  in the first run) and  $\text{Cl}^-$  accumulation in the anodic chamber maybe other reasons for the current density decreasing. The current of control MFC was below 0.02  $\text{mA}/\text{cm}^2$  (Fig. 2B).

The NaCl concentration in desalination chamber decreased from initial 2 g/L to about 1.5 g/L in two runs (Fig. 2C), whereas the conductivity of alkali production chamber increased from 3.5 to 4.5  $\text{mS}/\text{cm}$  (Fig. 2D). For the control MFC, the NaCl concentration in desalination chamber and conductivity in alkali production chamber changed slightly, likely caused by ion diffusion among membrane [14,26]. Therefore, besides alkali production, the salt concentration decreasing demonstrated another attractive function of our system.

The concentration profiles of  $\text{Na}^+$ ,  $\text{K}^+$ ,  $\text{HPO}_4^{2-}$  and  $\text{Cl}^-$  in alkali production chamber were illustrated in Fig. 3 to explain the performance change of BPMED–MFC in Fig. 2. Firstly, the pH dropping occurred in Fig. 2A, which was mainly due to two factors. (1) The  $\text{H}^+$  fluxed. Fig. 3 showed the migration of  $\text{K}^+$  from cathodic chamber. This indicated that the  $\text{H}^+$  also could transfer from cathodic chamber and (2) The  $\text{OH}^-$  lost. The  $\text{OH}^-$  could migrate from alkali production chamber to desalination chamber and cathodic chamber [25]. For example, the pH in desalination chamber increased about 0.8 in the first run. Secondly, as shown in Fig. 3, the concentration of  $\text{Na}^+$  in alkali production chamber increased from 0.7 to 1.2 g/L which should come from the  $\text{Na}^+$  transfer from desalination chamber

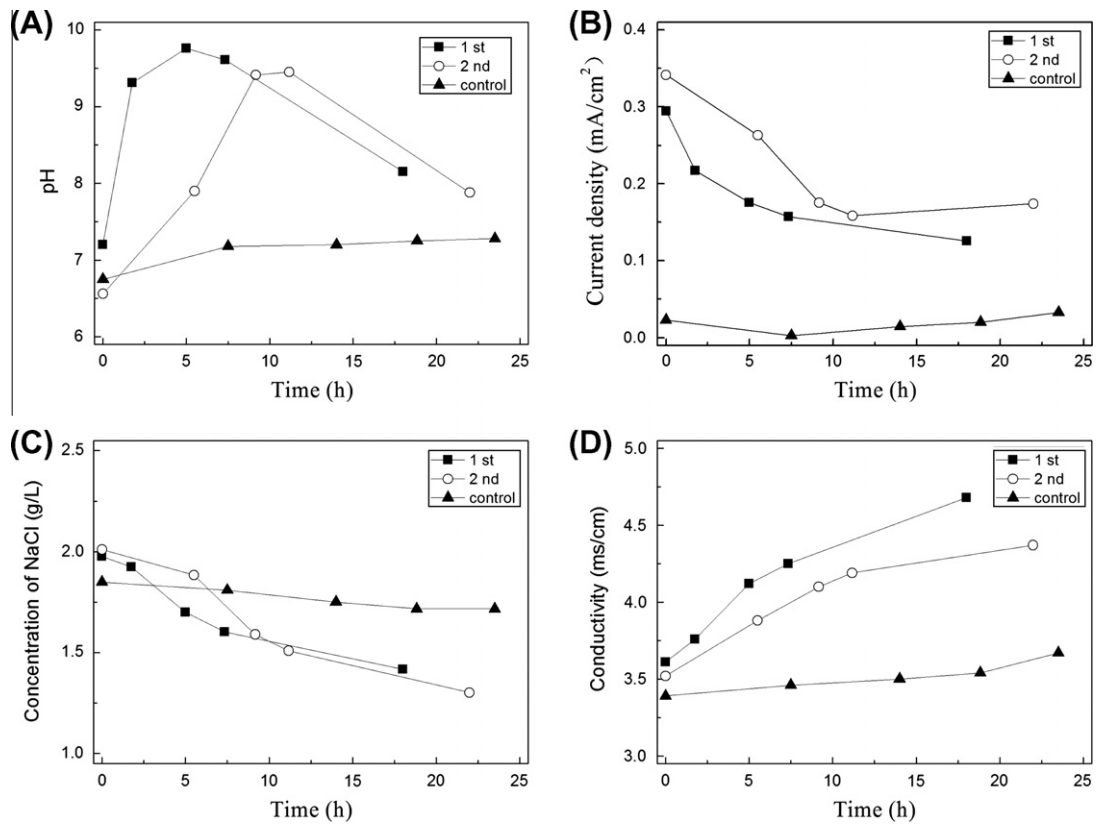


**Fig. 2.** Performance profiles of AEM-CEM-BPM configuration of BPMED-MFC (A), pH in alkali production chamber; (B), current density; (C), NaCl concentration in desalination chamber; and (D), solution conductivity in alkali production chamber.

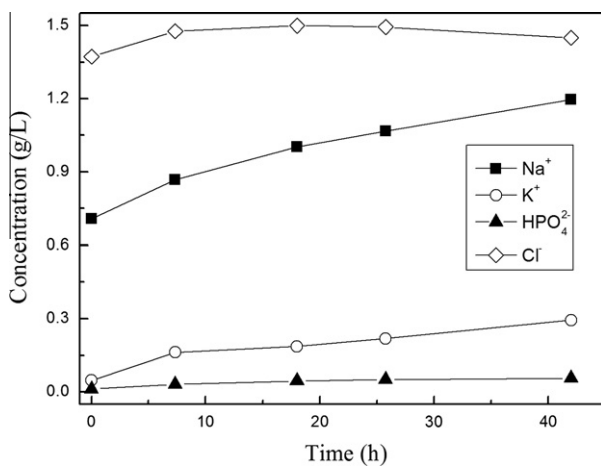


**Fig. 3.** Concentration of Na<sup>+</sup>, K<sup>+</sup>, HPO<sub>4</sub><sup>2-</sup> and Cl<sup>-</sup> in alkali production chamber of AEM-CEM-BPM configuration.

(Fig. 2C). Meanwhile, the Cl<sup>-</sup> and HPO<sub>4</sub><sup>2-</sup> in alkali production chamber did not change notably, which could maintain the purity of produced alkali.

On the other hand, as shown in Fig. 4, the power density was about 1150 mW/m<sup>2</sup>.

### 3.2. Effects of initial NaCl concentration and external resistance on alkali production

The solution conductivity and external resistance could significantly affect the performance of MFC [27]. As shown in Fig. 5A, un-

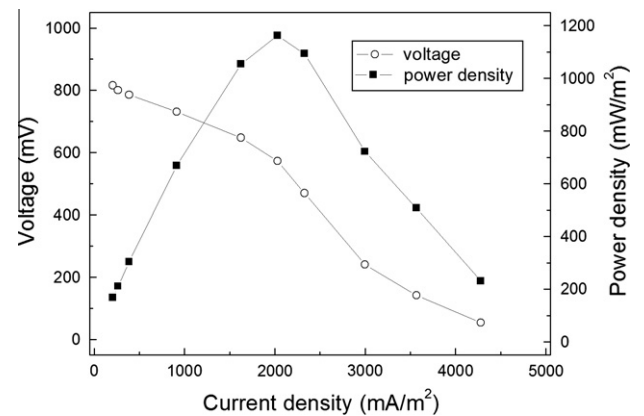


**Fig. 4.** Polarization curve and power output of AEM-CEM-BPM configuration at initial 2 g/L NaCl.

der 10  $\Omega$  external resistance, the maximum pH in the alkali production chamber increased from  $8.1 \pm 0.4$  to  $10.5 \pm 0.3$  when the concentration of NaCl in desalination chamber and alkali chamber elevated from 0.5 to 6 g/L. For 2 g/L NaCl in desalination chamber and alkali chamber, the maximum pH decreased from  $9.6 \pm 0.3$  to  $7.4 \pm 0.1$  in the alkali production chamber when the resistance increased from 10 to 1000  $\Omega$  (Fig. 5B). On the other hand, the coulombic efficiency was related to the solution conductivity and external resistance, which increased from  $22 \pm 2$  to  $33 \pm 5\%$  ( $n = 2$ ) as the increasing of NaCl concentration from 0.5 to 6 g/L and decreased from  $30 \pm 6$  to  $14 \pm 2\%$  ( $n = 2$ ) as the external resistance increasing from 10 to 1000  $\Omega$ .



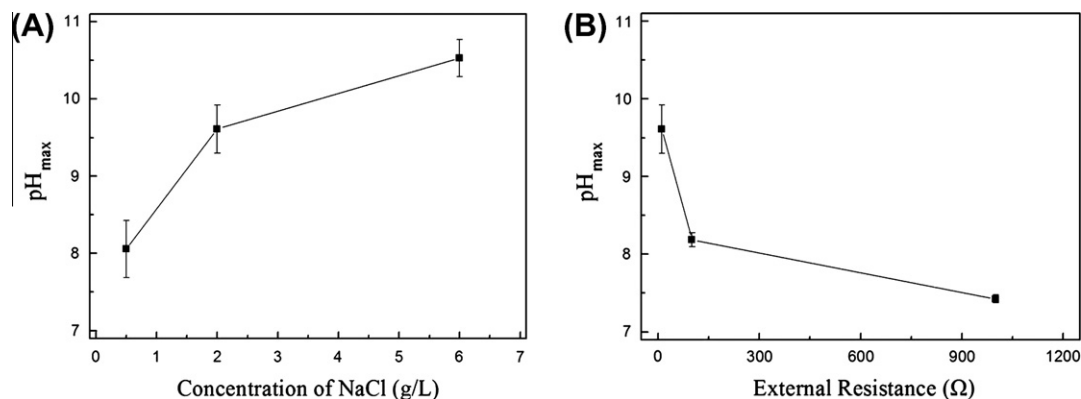


Fig. 5. Effects of concentration of NaCl (A) and external resistance and (B) on alkali production of AEM-CEM-BPM configuration.

### 3.3. Effects of applied voltage and system configuration on alkali production

It was reported that higher applied voltage in BPMED could increase product yield [26]. As shown in Fig. 6A, as the voltage increased from 0 to 0.5 V, the maximum pH raised from  $9.6 \pm 0.3$  to  $11.6 \pm 0.3$  in the alkali production chamber of AEM-CEM-BPM configuration. In the control MFC under the 0.5 V applied voltage, the pH in alkali production chamber did not change significantly within 25 h, as shown in the inset of Fig. 6A. The coulombic efficiency increased from  $30 \pm 6$  to  $80 \pm 8\%$  ( $n = 2$ ) when the applied voltage increased from 0 to 0.5 V.

On the other hand, the BPMED configuration also significantly affected their performance [26]. The addition of CEM and desalination chamber in AEM-CEM-BPM configuration increased the internal resistance comparing to AEM-BPM configuration. Therefore, the maximum pH ( $12.0 \pm 0.1$ ) in the alkali production chamber of AEM-BPM was slightly higher than that of AEM-CEM-BPM ( $11.6 \pm 0.2$ ) under the 0.5 V applied voltage, as shown in Fig. 6B. Meanwhile, the coulombic efficiency of AEM-BPM was  $78 \pm 8\%$  ( $n = 2$ ), comparable to that of AEM-CEM-BPM. However, without CEM,  $\text{OH}^-$  could easily transfer from alkali chamber to anodic chamber in AEM-BPM configuration, which caused pH drop more notably after 12 h than that of AEM-CEM-BPM configuration (Fig. 6B).

### 3.4. Biogas upgrading by the produced alkali solution

Alkali  $\text{CO}_2$  adsorption is one efficient technology for biogas upgrading. As shown in Table 1, the  $\text{CO}_2$  content decreased notably

after 20 min, for example, the final  $\text{CO}_2$  was even 0% at B4. In our study, both  $\text{CO}_2$  dissolving in water and reacting with  $\text{OH}^-$  led to the removal of  $\text{CO}_2$  in headspace. Firstly, the Henry's law coefficient of  $\text{CO}_2$  is  $0.035 \text{ mol}/(\text{L } 10^5 \text{ Pa})$  at  $25^\circ \text{C}$ , what means that 1 L water dissolves 0.78 L  $\text{CO}_2$  at  $10^5 \text{ Pa}$  of  $\text{CO}_2$  partial pressure. Therefore, even at initial pH 7.0, the final  $\text{CO}_2$  content also reduced to 7.96%, which was the same as the method of water scrubbing. [4] The dissolved  $\text{CO}_2$  also decreased the solution pH, as shown in Table 1. Secondly, alkali solution could react with  $\text{CO}_2$ , as shown in Eqs. (2) and (3). Since the final  $\text{CH}_4$  was higher than 90%, and even up to 100%, the produced alkali solution was suitable for biogas upgrading.



## 4. Discussion

### 4.1. The water dissociation mechanism in BPMED-MFC

The theory energy for water dissociation is calculated according to the Nernst equation (Eq. (4)), in which  $-\Delta G$  is the Gibbs free energy change for concentrating  $\text{H}^+$  and  $\text{OH}^-$  ions from their concentration in the interface of the bipolar membrane to the acid and base concentrations at the outer surface of the membrane; and  $a$  is the activity of  $\text{H}^+$  and  $\text{OH}^-$  ions, superscripts  $i$  and  $o$  refers to the interface and out surfaces of the BPM, respectively;  $E$  is the voltage drop across BPM;  $R$  is  $8.314 \text{ J}/(\text{mol K})$ ;  $T$  is the solution temperature, K;  $F$  is the faraday constant,  $96485.3 \text{ C}/\text{mol}$ . And, at

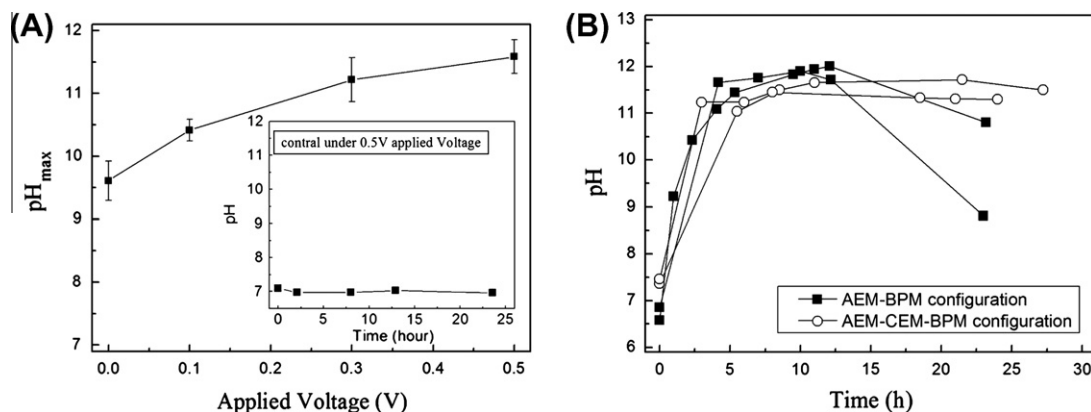


Fig. 6. Effects of applied voltage (A) and system configuration and (B) on alkali production.

**Table 1**

The performance of biogas upgrading with alkali solution.

	Initial pH	Final pH	Final CO <sub>2</sub> content (%)
B0	7.0	5.1 ± 0.1	7.96 ± 0.48
B1	9.6	5.6 ± 0.2	7.82 ± 0.36
B2	10.3	6.3 ± 0.4	6.93 ± 0.06
B3	11.2	6.7 ± 0.4	4.30 ± 0.28
B4	11.6	9.7 ± 0.1	0.00 ± 0.00

298.15 K, the 0.828 V is the potential drop of BPM for 1 mol/L ideal alkali and acid production [11,12].

$$\Delta G = nEF = RT \ln \frac{a_H^i \times a_{OH}^i}{a_H^o \times a_{OH}^o} \quad (4)$$

$$E = \frac{2.3 \times R \times T \times \Delta pH}{F} \quad (5)$$

Moreover, when the  $\Delta pH$  is defined as the pH difference of alkali solution and acidic solution, and  $a_H^i \times a_{OH}^i$  is equal to  $k_w$ , and  $a_H^o \times a_{OH}^o$  is equal to  $(k_w - \Delta pH)$ , the Eq. (5) could deduce from Eq. (4). Therefore, water dissociation of BPM is controlled by the voltage drop among the membrane [11,20]. The voltage drop of BPM is about 0.2 V for MFC with BPM as separator [21,22]. When 0.2 V is applied in Eq. (3), the maximum  $\Delta pH$  (3.4) across BPM is similar to ours ( $\Delta pH$  around 3 in Fig. 2A), which supports our BPMED–MFC concept in theory. Nevertheless, since the water dissociation is also related to the diffusion coefficients of salt ions and water, the ion mobilities in the membrane, the fixed charge density of the membrane, etc. [10], extensive works are still required to investigate the mechanism in BPMED–MFC.

On the other hand, the current density is also an important factor for water dissociation in BPM. The water dissociation efficiency decreased from 70% to 0% as the current density decreased from 10 to 0 mA/cm<sup>2</sup> [28]. In our study, the experimental results also supported this trend. For example, as the applied voltage increased from 0 to 0.5 V, the maximum current density increased from 0.3 to 0.7 mA/cm<sup>2</sup>. Coincidentally, the maximum pH in alkali production chamber also increased from 9.6 to 11.6. Meanwhile, our current densities were also comparable to other studies (between 0.45 and 0.84 mA/cm<sup>2</sup>) [24].

#### 4.2. The perspective of BPMED–MFC

Recently, Rabaey et al. also proposed alkali production in cathodic chamber of MFC, and the maximum pH was 13.8. However, since high extra voltage (1.77 V) was applied, constant anodic potential had to be set as –0.2 V or –0.3 V to maintain microbial activity and stable performance [18]. The authors also claimed that calcium scaling and gas bubble in cathode decreased the performance of alkali production. Contrarily, in our study, the alkali was produced in a separate chamber, which could avoid those problems. Furthermore, due to the functional group degradation of BPM and the limitation of electroosmosis and co-ion/counter-ion migration, it was also not wise to operate at very high pH in BPMED [9,29]. So, it is rather clear that BPMED–MFC is suitable and beneficial to produce alkali.

The cost is one of critical parameters to assess the biogas upgrading technologies. Firstly, as reviewed by Petersson and Wellinger, the cost of chemical scrubber was lower than other technologies especially at high operational capacity [4]. For chemical scrubber, the cost for alkali scrubber is lower than amine scrubber as it can simultaneously adsorb CO<sub>2</sub> and H<sub>2</sub>S. Secondly, the BPMED technology has been demonstrated both economic and environmental benefits in amine regeneration, organic acid production and CO<sub>2</sub> separation [9,13,25,26]. Moreover, the invest-

ment and operational cost would be lower with the development of BPMED. Thirdly, the power source used in this work can also be substituted by an additional microbial fuel cell, which is similar to the work proposed by Sun et al. for hydrogen production [30]. Thus, the alkali production from BPMED–MFC could be an attracting technology for biogas upgrading. Nevertheless, extensive investigations are required to make MFC work more applicable [15,16,30].

BPMED has also been used to produce organic acid and realize non-aqueous solvent dissociation (methanol and ethanol), which are valuable for industrial application [31–33]. Therefore, it is expected the multi-function of BPMED powered by MFC could be an elegant and sustainable approach to extend the application of bipolar membrane electro dialysis process and microbial fuel cell.

## 5. Conclusions

In this study, BPMED powered by MFC was demonstrated successfully for alkali production and *in situ* electricity utilization. The produced alkali solution was suitable for biogas upgrading. The main outcomes were:

- The maximum pH in the alkali production chamber without applied voltage and with 0.5 V applied voltage was 9.8 and 11.6, respectively.
- With higher NaCl concentration, bigger applied voltage and lower external resistance, the alkali yield increased.
- BPMED–MFC system also showed the performance of desalination (from 2.0 to 1.5 g/L NaCl).
- The produced alkali solution could notably reduce CO<sub>2</sub> content and upgrade CH<sub>4</sub> even to 100%.

## Acknowledgements

The authors would like to acknowledge the financial support from Hundred-Talent Program of CAS and the Fundamental Research Funds for the Central Universities (Grant No. WK2060190007).

## References

- [1] Ryckebosch E, Drouillon M, Vervaeren H. Techniques for transformation of biogas to biomethane. *Biomass Bioenerg* 2011;35:1633–45.
- [2] Chandra R, Takeuchi H, Hasegawa T. Hydrothermal pretreatment of rice straw biomass: a potential and promising method for enhanced methane production. *Appl Energ* 2012;94:129–40.
- [3] Murphy JD, Power N. Technical and economic analysis of biogas production in Ireland utilising three different crop rotations. *Appl Energ* 2009;86:25–36.
- [4] Petersson A, Wellinger A. Biogas upgrading technologies – developments and innovations. IEA-Task 2009;37:20.
- [5] Deng L, Hägg M-B. Techno-economic evaluation of biogas upgrading process using CO<sub>2</sub> facilitated transport membrane. *Int J Greenhouse Gas Control* 2010;4:638–46.
- [6] Lantela J, Rasi S, Lehtinen J, Rintala J. Landfill gas upgrading with pilot-scale water scrubber: performance assessment with absorption water recycling. *Appl Energ* 2012;92:307–14.
- [7] Mohseni F, Magnusson M, Görling M, Alvfors P. Biogas from renewable electricity – increasing a climate neutral fuel supply. *Appl Energ* 2012;90:11–6.
- [8] Lombardina L, Corti A, Carnevale E, Baciocchi R, Zingaretti D. Carbon dioxide removal and capture for landfill gas up-grading. *Energ Procedia* 2011;4:465–72.
- [9] Huang C, Xu T. Electrodialysis with bipolar membranes for sustainable development. *Environ Sci Technol* 2006;40:5233–43.
- [10] Strathmann H, Krol JJ, Rapp HJ, Eigenberger G. Limiting current density and water dissociation in bipolar membranes. *J Membr Sci* 1997;125:123–42.
- [11] Tanaka Y. Ion exchange membranes: fundamentals and applications. Elsevier Science; 2007.
- [12] Strathmann H. Ion-exchange membrane separation processes. Elsevier Science; 2004.
- [13] Eisaman MD, Alvarado L, Larner D, Wang P, Garg B, Littau KA. CO<sub>2</sub> separation using bipolar membrane electro dialysis. *Energ Environ Sci* 2011;4:1319–28.

- [14] Xu T, Huang C. Electrodialysis-based separation technologies: a critical review. *AIChE J* 2008;54:3147–59.
- [15] Harnisch F, Schroder U. From MFC to MXC: chemical and biological cathodes and their potential for microbial bioelectrochemical systems. *Chem Soc Rev* 2010;39:4433–48.
- [16] Logan BE, Hamelers B, Rozendal R, Schröder U, Keller J, Freguia S, et al. Microbial fuel cells: methodology and technology. *Environ Sci Technol* 2006;40:5181–92.
- [17] Cao X, Huang X, Liang P, Xiao K, Zhou Y, Zhang X, et al. A new method for water desalination using microbial desalination cells. *Environ Sci Technol* 2009;43:7148–52.
- [18] Rabaey K, Butzer S, Brown S, Keller Jr, Rozendal RA. High current generation coupled to caustic production using a lamellar bioelectrochemical system. *Environ Sci Technol* 2010;44:4315–21.
- [19] Zhao F, Harnisch F, Schröder U, Scholz F, Bogdanoff P, Herrmann I. Challenges and constraints of using oxygen cathodes in microbial fuel cells. *Environ Sci Technol* 2006;40:5193–9.
- [20] ter Heijne A, Hamelers HVM, de Wilde V, Rozendal RA, Buisman CJN. A bipolar membrane combined with ferric iron reduction as an efficient cathode system in microbial fuel cells. *Environ Sci Technol* 2006;40:5200–5.
- [21] ter Heijne A, Hamelers HVM, Buisman CJN. Microbial fuel cell operation with continuous biological ferrous iron oxidation of the catholyte. *Environ Sci Technol* 2007;41:4130–4.
- [22] Rozendal R, Sleutels T, Hamelers H, Buisman C. Effect of the type of ion exchange membrane on performance, ion transport, and pH in biocatalyzed electrolysis of wastewater. *Water Sci Technol* 2008;57:1757–62.
- [23] Harnisch F, Schröder U, Scholz F. The suitability of monopolar and bipolar ion exchange membranes as separators for biological fuel cells. *Environ Sci Technol* 2008;42:1740–6.
- [24] Chen S, Liu G, Zhang R, Qin B, Luo Y. Development of the microbial electrolysis desalination and chemical-production cell for desalination as well as acid and alkali productions. *Environ Sci Technol* 2012;46:2467–72.
- [25] Zhang F, Huang C, Xu T. Production of sebacic acid using two-phase bipolar membrane electrodialysis. *Ind Eng Chem Res* 2009;48:7482–8.
- [26] Huang C, Xu T. Regeneration of flue-gas desulfurizing agents by bipolar membrane electrodialysis. *AIChE J* 2006;52:9.
- [27] Fan Y, Sharbrough E, Liu H. Quantification of the internal resistance distribution of microbial fuel cells. *Environ Sci Technol* 2008;42:8101–7.
- [28] Bauer B, Gerner FJ, Strathmann H. Development of bipolar membranes. *Desalination* 1988;68:279–92.
- [29] Gineste JL, Pourcelly G, Lorrain Y, Persin F, Gavach C. Analysis of factors limiting the use of bipolar membranes: a simplified model to determine trends. *J Membr Sci* 1996;112:199–208.
- [30] Sun M, Sheng GP, Zhang L, Xia CR, Mu ZX, Liu XW, et al. An MEC–MFC-coupled system for biohydrogen production from acetate. *Environ Sci Technol* 2008;42:8095–100.
- [31] Onishi N, Osaki T, Minagawa M, Tanioka A. Alcohol splitting in a bipolar membrane and analysis of the product. *J Electroanal Chem* 2001;506:34–41.
- [32] Huang C, Xu T, Zhang Y, Xue Y, Chen G. Application of electrodialysis to the production of organic acids: state-of-the-art and recent developments. *J Membr Sci* 2007;288:1–12.
- [33] Li Q, Huang C, Xu T. Alcohol splitting for the production of methyl methoxyacetate: integration of ion-exchange with bipolar membrane electrodialysis. *J Membr Sci* 2011;367:314–8.